Fuel 252 (2019) 598–611

Contents lists available at ScienceDirect

Fuel

journal homepage: www.elsevier.com/locate/fuel

Full Length Article

The effect of fuel composition on particulate emissions from a highly boosted GDI engine – An evaluation of three particulate indices

Felix C.P. Leach[a,*], Richard Stone[a], David Richardson[b], Andrew G.J. Lewis[c], Sam Akehurst[c], James W.G. Turner[c], Varun Shankar[c,d], Jasprit Chahal[d], Roger F Cracknell[d], Allen Aradi[e]

[a] Department of Engineering Science, University of Oxford, UK
[b] Powertrain Research, Jaguar Land Rover, UK
[c] Powertrain & Vehicle Research Centre, University of Bath, UK
[d] Shell Global Solutions, UK
[e] Shell Global Solutions, USA

ARTICLE INFO

Keywords:
PN
Particulate
Fuel effects
GDI
Downsizing
Boost
PM index
PN index

ABSTRACT

Gasoline Direct Injection (GDI) engines equipped with a turbocharger or supercharger (known as boosted engines) have achieved significant market penetration due to their advantages in reducing CO_2 emissions compared to Port Fuel Injection (PFI) engines. These engines are known to emit particulate matter and recent studies have characterized these emissions. Fuel composition is known to have an impact on Particle Number (PN) emissions from GDI engines, however its effect on emissions from highly boosted engines is not known.

In this work, 10 different fuels have been tested on an extremely highly boosted engine (at up to 35 bar BMEP) at several different operating conditions both unboosted and boosted and the PN emissions and size distributions have been measured using a Cambustion DMS500. The applicability of three previously developed indices linking fuel composition to PN emissions is tested with the results from these fuels.

The results show that the PM index is a good predictor of PN emissions from this engine for all fuels at all operating points (unboosted and boosted). The Moriya and PN indices predict the PN emissions using fuels that are market representative, but are poor predictors of PN emissions over all of the fuels tested. Very small accumulation mode particle sizes of around 30 nm have been noted from all fuels at boosted conditions, which has relevance to future legislation and after treatment.

1. Introduction

Over 40% of the light duty vehicle market in Europe now comprises of Gasoline Direct Injection (GDI) engines [1]. Such engines offer an advantage in reducing CO_2 emissions and decreasing fuel consumption, compared to Port Fuel Injection (PFI) engines, however they are known to emit more Particulate Matter (PM) emissions, notably Particle Number (PN) emissions, than their PFI counterparts [2]. Downsized GDI engines, so called because they offer the same power output for a smaller engine displacement, achieve their downsized nature by pressurising the inlet air, usually through turbocharging or supercharging. These downsized engines further reduce CO_2 emissions and decrease vehicle fuel consumption by reducing friction and operating engines at higher Brake Mean Effective Pressures. These engines are increasingly available in the market [3].

GDI engines emit PN which usually have a logbinormal distribution [4]. These two lognormally distributed modes are known as the nucleation mode (usually consisting of volatile and semi-volatile particles with a diameter of less than 30 nm) and the accumulation mode (solid particles with other species adsorbed onto them of diameters between 40 nm and 200 nm). PN emissions from GDI engines have been extensively studied [2,4–6] and an increasing number of studies are now reporting PN emissions from boosted GDI engines [7–10] and small particle sizes have been noted in these studies. PN emissions from GDI

Abbreviations: AFR, air fuel ratio; BMEP, brake mean effective pressure; DHA, detailed hydrocarbon analysis; DMS, differential mobility spectrometer; DVPE, dry vapour pressure equivalent; EBP, exhaust back pressure; EGR, exhaust gas recirculation; GDI, gasoline direct injection; GEM, gasoline ethanol and methanol; KLSA, knock limited spark advance; NEDC, new European drive cycle; MON, motor octane number; PAH, polycyclic aromatic hydrocarbons; PIONA, paraffins, isoparaffins, olefins, naphthenes, and aromatics; PM, particulate matter; PMP, particle measurement protocol; PN, particle number; RON, research octane number; RVP, Reid Vapour pressure; THC, total hydrocarbon

* Corresponding author.
E-mail address: felix.leach@eng.ox.ac.uk (F.C.P. Leach).

https://doi.org/10.1016/j.fuel.2019.04.115
Received 15 October 2018; Received in revised form 11 January 2019; Accepted 18 April 2019
Available online 06 May 2019
0016-2361/

engines are limited by the Euro 6 legislation to 6×10^{11} #/km.

1.1. Effect of fuel composition on PN emissions from GDI engines

It is known that the composition of gasoline will effect PN emissions from GDI engines [11]. A number of recent works have focussed on links between fuel composition and particulate emissions from those fuels [12,13]. Aikawa et al. developed an index (the PM index – Eq. (1)) for PFI engines linking PN emissions to fuel composition [14,15] showing a good correlation. Aikawa showed that the PN emissions were dependent on a fuel's Double Bond Equivalent (DBE – Eq. (2)) and its Vapour Pressure (VP) evaluated at a temperature of 443 K. The PM index is defined in Eq. (1):

$$PM\ index = \sum_{i=1}^{n} \left[\frac{DBE_i + 1}{VP_i} \right] W_{ti} \quad (1)$$

VP_i is the vapour pressure of an individual component at 443 K, W_{ti} is the mass fraction of each component, and *DBE* for each component is defined from Eq. (2):

$$DBE = \frac{2C^{\circ} - H^{\circ} + 2}{2} \quad (2)$$

where C and H are the number of Carbon and Hydrogen atoms respectively present in an organic compound. DBE is a measure of how unsaturated a hydrocarbon component is – i.e. how many pairs of hydrogen atoms would need to be added to convert the component into an alkane, while retaining the same number of carbon atoms – for example toluene ($C_6H_5.CH_3$) has a DBE of 4 and its corresponding alkane is heptane (C_7H_{16}), which has a DBE of 0.

This dependence of PN emissions on VP and DBE is not surprising, as the VP of a fuel will affect its evaporative performance; in general fuels with a higher VP will evaporate more readily when injected into the cylinder, resulting in a more homogeneous mixture at ignition and hence lower PN emissions. In addition the hydrocarbon species present in the fuel will affect the formation of particulates; particle formation occurs initially by coalescence of polycyclic aromatic hydrocarbons (PAHs) [16] – the presence of these aromatic compounds in the fuel will therefore promote particle formation and hence increase PN emissions – DBE is a measure of this. Unfortunately calculation of the PM index requires a detailed compositional breakdown (a Detailed Hydrocarbon Analysis (DHA) – ASTM D5134 [17]) of the fuel in order to calculate the VP contribution from each component at 443 K, which limits its use outside of detailed fuels research.

To overcome this calculation difficulty Aikawa's work was further developed previously by some of this work's authors into the PN index for GDI engines [18,19]. The PN index can be calculated from data available on a standard fuel data sheet (DVPE [20] and PIONA analysis – ASTM D1319 [21]) and is defined below in Eq. (3):

$$\text{PN index} = \frac{\sum_{i=1}^{n} [DBE_i + 1] V_i}{DVPE(\text{kPa})} \quad (3)$$

here *DVPE* is Dry Vapour Pressure Equivalent, V_i is the volume fraction of each component, and *DBE* as in Eq. (2).

Of course the test methods for the parameters in the PN index have an error associated with them, as specified in the various legislative methods [22]. These can be cascaded into an overall error associated with the PN index. These errors have been included wherever the PN index is plotted in this work.

An alternative, even more simple method, was developed by Moriya [23]. This work developed two indices relating the distillation characteristics of the fuel to its expected particulate emissions.

$$Moriya\ index = -0.0647 \times E170 - 0.0324 \times E130 + 9.92405 \quad (4)$$

$$Simplified\ Moriya\ index = -0.0757 \times E150 + 7.8511 \quad (5)$$

where EXXX is the percentage of the fuel evaporated at xxx °C.

The PN index was shown to be a reliable predictor of PN emissions from GDI engines at steady state, however transient behaviour was more complex, and the trends of the PN index were masked by other effects during transient operation of an engine. The PM index and Moriya indices have shown themselves to be generally applicable as well – with some initial comparisons between indices undertaken in [24]. Other work has also been undertaking linking fuel composition to particulate emissions; Barrientos et al. showed good results using an Oxygen Extended Sooting Index (OESI) which they developed using a fuel's C:H:O ratio and its smoke point [25]. Other indices include those developed by General Motors [12] and Menger and Wittmann [13].

Whether the PM, PN, and Moriya indices are relevant to particulate emissions from highly boosted engines will be examined in this work. The results section will present the results from the engine testing, followed by a discussion of the results in the context of these three particulate indices.

2. Experimental methodology

PN emissions were measured from an engine running at a variety of operating conditions including highly boosted operating points, using 10 different fuels in order to examine the effect of fuel composition on PN emissions from a highly boosted engine. These PN emissions have been evaluated against the three indices calculated for the fuels.

2.1. Engine

The "Ultraboost" engine used in this work is able to operate at BMEPs of up to 35 bar. Details of this engine are in Table 1. A detailed description of the engine and its design is available in Turner et al. [26]. During this work the engine was not fitted with a turbocharger or a supercharger, so inlet and exhaust conditions were controlled by an external boosting rig and a back-pressure valve which simulated the inlet and exhaust pressures that would be provided by the turbocharger and/or supercharger.

2.2. Instrumentation

PN emissions were measured using a Cambustion DMS500 (DMS). The DMS uses electrical charge to drag ratio to measure a particle's size (expressed as an electrical mobility diameter) and to count the total number of particles; more information about the DMS and its operating principle is available in Reavell et al. [27]. Braisher et al. [28] have shown that PN emissions as measured by a DMS correlate closely with PN emissions measured in accordance with a legislatively compliant particle counting system. The DMS analysis and sampling methodology used here are described in [10].

2.3. Engine test points

A 66-point experimental matrix was run consisting of four basic engine operating conditions. These range from a low speed/load point (1250 rpm/3.77 bar BMEP) which is a New European Drive Cycle (NEDC) minimap point (the minimap point is a single operating point representative of a portion of the NEDC), to the full load curve at three

Table 1
Specifications of the UB100 engine.

Type	Inline 4 cylinder
Bore × Stroke	83 × 92 mm
Displacement	1991 cm^3
Valves per cylinder	2 intake, 2 exhaust
Compression ratio	9:1
Maximum fuel pressure	200 bar
Peak BMEP	35 bar

Table 2
Experimental test points.

Test point	Speed (rpm)	Load (bar BMEP)	Inlet Air T (°C)	EBP	λ	P_{inj} (bar)	EGR (%)
1	2000	Max*	40	Low	1.0	200	0/10†
2	1250	3.77	20/40†	Low	1.0	60	0
3	3000	Max*	60	Low/High†	1.0	200	10
4	4000	Max*	40	High	1.0/0.875†	200	10

* Max BMEP constrained by knock and P_{max} limits.
† Indicates both conditions tested separately.

different engine speeds (2000, 3000, and 4000 rpm). This enables not only the measurement of PN emissions at highly boosted conditions, but also, through a naturally aspirated operating point, verification with existing data and knowledge.

A more complete description of the test matrix is given in [10]. Details of the engine test points are shown in Table 2:

The maximum BMEP at full load was limited by knock and maximum in-cylinder pressure (P_{max}). The full load test points were taken at 10 ignition timings, Knock Limited Spark Advance (KLSA) and 9 retardations in increments of 1 CAD. Test point 2 (1250 rpm/3.77 bar BMEP) was measured at three injection timings (baseline and ± 10 CAD) and seven ignition timings (at the baseline injection timing).

The engine was run fully warm, after a period of stabilization, and the test points were always run in the same order (that shown in Table 2). DMS data, down-sampled to 1 Hz from 10 Hz, was logged for at least 30 s and the mean and standard deviation of this 1 Hz log is presented in this work.

2.4. Test fuels

PN emissions from 10 different fuels were measured in this work, supplied by Shell Global Solutions. These fuels were not blended with particulate measurements specifically in mind, but rather for their effects on engine combustion which have already been reported [29,30]. The base fuel was an EN228 compliant gasoline representative of UK market fuel (containing up to 5% v/v ethanol); the other fuels were all blended with a specific purpose in mind. Fuels A-D were blended to test the sensitivity of the engine to RON and MON, so represent a "deconvolved" RON-MON matrix with broadly independent RON and MON as far as was possible within blending limits; Fuels A and B contain MTBE, an oxygenate. Fuels E and F were blended to test the impact of Laminar Flame Speed on the engine combustion, with Fuel E having a high laminar flame speed, and Fuel F a low laminar flame speed. At the full load operating points, Fuel E gave a ~10–14% decrease in 10–50% burn duration compared to Fuel F. Fuel G is a special fuel with an artificially boosted RON. Fuels H and I are fuels that could be available in the market, with Fuel H being an EN228 compliant fuel (containing up to 5% v/v ethanol), with the minimum RON required (95) and Fuel I is similar to a market "premium" gasoline with slightly higher octane and a high DVPE, so representative of a winter grade. Distillation curves are shown in Refs. [29,30] (Figs. 3 and 2 in those papers respectively). Fuel specifications along with calculations of PN, PM, and Moriya indices are shown in Table 3, and compositional breakdown calculation from PIONA analysis is shown in Table 4. Unfortunately a DHA was not available for Fuel I so the PM index was not able to be calculated for this fuel.

3. Results

The results reported here were part of a larger set of experiments testing 14 different fuels, which have been reported elsewhere [10,29–31], which also contain a more detailed discussion of the experimental methodology. The fuels were tested in batches in order GHI, oil change, ABCD, oil change, EF. After each oil change the engine was subjected to a de-greening procedure to run it in. The Base fuel was tested at the start and end of the tests, noted as Base 1 and Base 2 in the results, and provides a measure of repeatability, which is generally very good. The other fuels were only tested once. The PN emissions reported in this work are presented as digitally filtered results with a count efficiency of 50% at 23 nm and 90% at 41 nm; this replicates the effect of the PMP protocol, the legislatively compliant methodology for counting particles in Europe [32]. The size distributions presented are unfiltered, and the mean and standard deviation of the 1 Hz DMS data over an individual test point is presented. When the size distributions are considered it will be noted that the effect of this filtering is to discount large numbers of the particles emitted, certainly the nucleation mode (which would be mostly removed by a catalyst) but in some cases a substantial part of the accumulation mode as well.

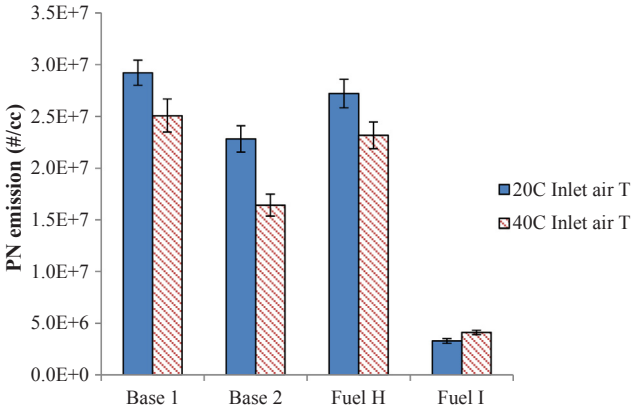

Fig. 1. PN emissions from market representative fuels at 1250 rpm/3.77 bar BMEP – showing the effect of varying inlet air temperature. The error bars correspond to ± σ.

3.1. Market representative fuels

Three fuels were tested that are representative of fuels available in the EU market both winter and summer grades. As mentioned above, the Base fuel was a standard EN228 compliant fuel, Fuel H is an EN228 compliant fuel with the minimum RON required, and Fuel I is a slightly higher octane fuel with a high DVPE, so representative of winter grade.

3.2. 1250 rpm/3.77 bar BMEP (Test point 2)

Fig. 1 shows the PN emissions from the market representative fuels at 1250 rpm/3.77 bar BMEP (an NEDC minimap point) and Fig. 2 the size distribution of these emissions at an inlet temperature of 20 °C. This test point serves as a crosscheck with existing results as the engine is not boosted at all at this very light load operating point. The PN emissions behave as would be expected, with a decrease in PN emissions noted with an increase in inlet air temperature due to the higher temperatures promoting a more homogeneous mixture and hence lower PN. Fuel I, however, does not show a reduction in PN as inlet air temperature is increased, emitting very low levels of PN overall. Fuel I has a very high

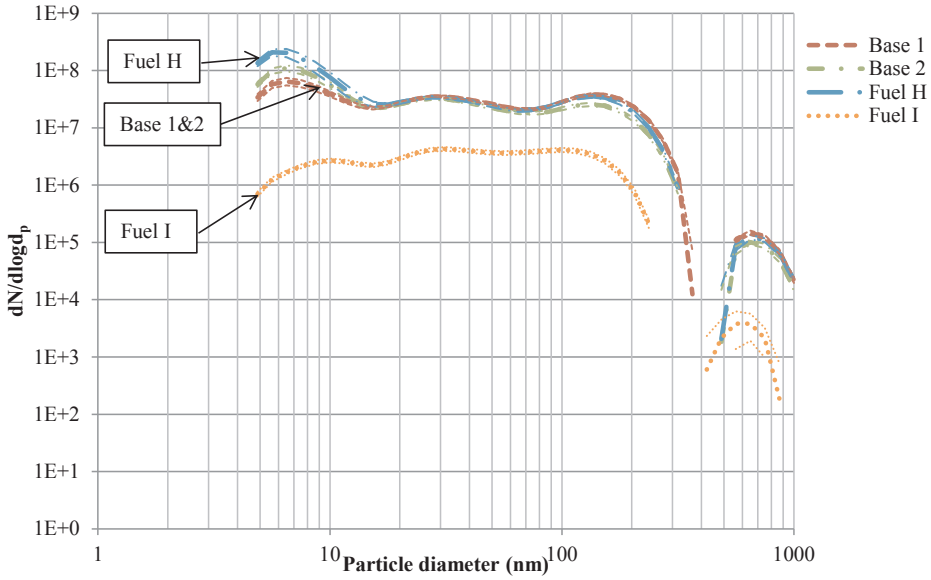

Fig. 2. PN size distributions from market representative fuels at 1250 rpm/3.77 bar BMEP, (Inlet air T = 20 °C) – this corresponds to the solid bars on Fig. 1. Note the logarithmic scale on the ordinate. The error bands correspond to ± σ.

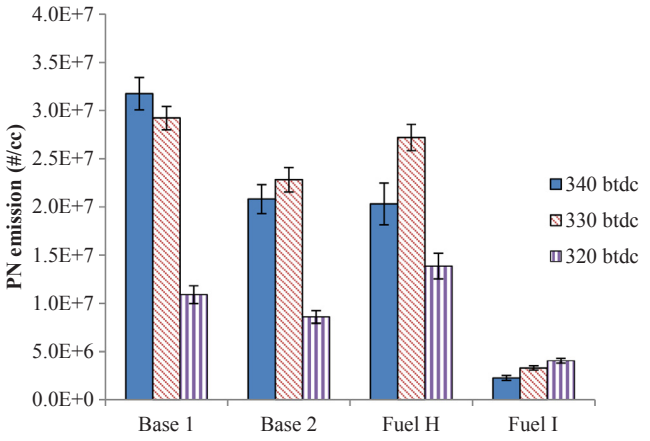

Fig. 3. PN emissions from market representative fuels at test point 2 – showing the effect of varying fuel injection timing. The error bars correspond to ± σ.

vapour pressure (VP) (the highest of all the fuels tested) suggesting that the mixture formed by Fuel I is already fully evaporated due to its high VP, and hence further evaporation is not promoted by increasing the inlet air temperature. Indeed the increase in inlet temperature might be causing rapid evaporation of Fuel I upon injection (possibly even flash-evaporation) leading to a more locally rich, less homogeneous mixture, and hence an overall increase in PN emissions – indeed above a certain level, flash-evaporation can cause spray collapse and a decrease in mixture homogeneity [33]. Looking at Fig. 2 gives a greater understanding, Fuels Base, H, and I show a standard bi-modal distribution – nucleation and accumulation modes – with peaks at around 30 nm and 150 nm. A third mode, the so-called coarse mode, is observed at around 700 nm. It is likely that this mode mostly consists of re-entrained particles from the exhaust. This feature is present in all of the particle size spectra presented in this paper with slightly varying magnitudes – but always around 2–3 orders of magnitude lower than the other particulates, although it is not always visible in subsequent plots due to scaling.

Fig. 3 shows the PN emissions from the market representative fuels at 1250 rpm/3.77 bar BMEP as the fuel injection timing is varied. The Base fuel and Fuel H show higher levels of PN emissions at 340 and 330 CAD btdc and then a significant decrease at 320 CAD btdc. This suggests that, as has been observed before, at these very early injection timings, the fuel spray is impinging on the piston and subsequently burning as a pool fire, leading to higher levels of PN. At 320 CAD btdc injection, the piston has moved sufficiently far from tdc such that the

Table 3
Test fuel specification.

Fuel	RON (−)	MON (−)	DVPE (kPa)	FBP (°C)	E150 (%)	C (% m/m)	H (% m/m)	O (% m/m)	PN index* (1/kPa)	PN index** (1/kPa)	PM index (1/kPa)	Moriya index***(%)
A	103.3	95	26.1	177	96	7.15	14.45	0.17	6.57	6.61	0.55	0.57
B	101.4	88.8	68.0	176	95	6.40	11.17	0.11	3.97	3.99	1.01	0.68
C	92.8	90.7	30.5	193	93	7.41	15.94	0.00	4.23	4.31	0.49	0.82
D	88.6	87.3	32.9	190	92	7.31	15.64	0.00	4.03	4.12	0.53	0.91
E	95.1	82.2	28.7	138	98	6.68	12.38	0.00	10.41	10.41	0.99	0.44
F	104.2	92.6	23.3	139	98	6.94	12.46	0.00	11.14	11.14	1.04	0.42
G	111.6	101.2	57.4	192	98	7.10	11.80	0.00	5.69	5.69	1.00	0.44
H	95.1	85.0	53.1	189	88	6.20	11.48	0.10	4.64	4.67	1.32	1.18
I†	98.7	86.5	97.4	173	95	6.28	11.23	0.00	2.64	n/k	n/k	0.66
Base	97	85.3	75.0	188	92	6.05	11.11	0.10	3.30	3.33	1.10	0.87

* Calculated from PIONA (ASTM D1319) analysis.
** Calculated from DHA.
*** Simplified Moriya index by Eq. (5).
† A DHA was unavailable for Fuel I.

Table 4
Detailed test fuel composition.

Fuel	Paraffins (% v/v)	Isoparaffins (% v/v)	Olefins (including dienes) (% v/v)	Naphthenes (% v/v)	Aromatics (% v/v)	Oxygenates (% v/v)	Unknowns (% v/v)
A	1.26	65.25	0.34	1.28	17.57	13.97	0.33
B	7.83	28.71	11.49	2.06	39.11	10.45	0.35
C	3.11	85.80	1.10	1.77	6.87	0.00	1.35
D	6.88	80.64	1.25	1.65	7.83	0.00	1.75
E	6.39	8.65	16.86	30.19	37.92	0.00	0.01
F	0.38	46.66	17.22	0.20	35.53	0.00	0.00
G	0.08	43.25	0.00	0.00	56.67	0.00	0.00
H	9.81	39.34	7.29	4.75	33.64	4.92	0.25
I	10.77	35.17	16.06	2.71	34.73	0.00	0.56
Base	11.37	32.76	14.25	3.93	32.38	4.91	0.40

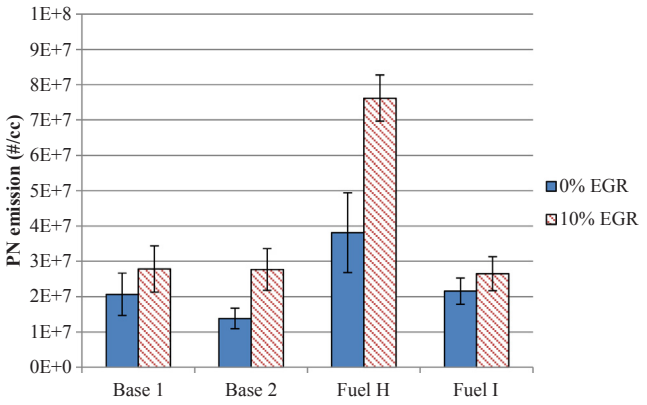

Fig. 4. PN emissions from market representative fuels at 2000 rpm/full load – showing the effect of adding EGR. The error bars correspond to ± σ.

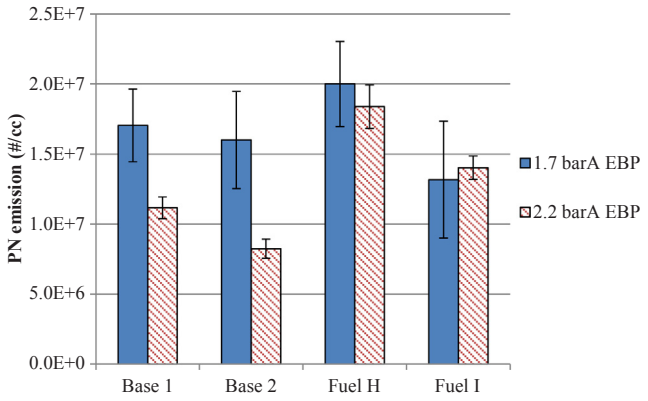

Fig. 6. PN emissions from market representative fuels at 3000 rpm/full load – showing the effect of increasing exhaust back pressure. The error bars correspond to ± σ.

fuel does not impinge, and evaporates fully leading to lower levels of PN emitted. Fuel I does not follow this trend and has very low levels of PN at all three injection timings. As noted above, Fuel I also has the highest VP of any of the fuels tested, suggesting that even at the earliest injection timing it is evaporating before it has a chance to impinge on the combustion chamber surfaces. This is further supported by the minor increase in PN emissions as the injection is advanced as there is slightly less time for a homogeneous mixture to form and hence a slight increase in PN.

3.3. 2000 rpm/full load (Test point 1)

Fig. 4 shows the PN emissions from the market representative fuels at 2000 rpm and full load, as the cooled, external EGR is increased from 0 to 10 % and Fig. 5 shows the size distributions from the 10% EGR case. These fuels all show an increase in PN with EGR, attributed to the decrease in exhaust temperature with EGR reducing post-flame oxidation. The size distributions show the skew towards very small particles

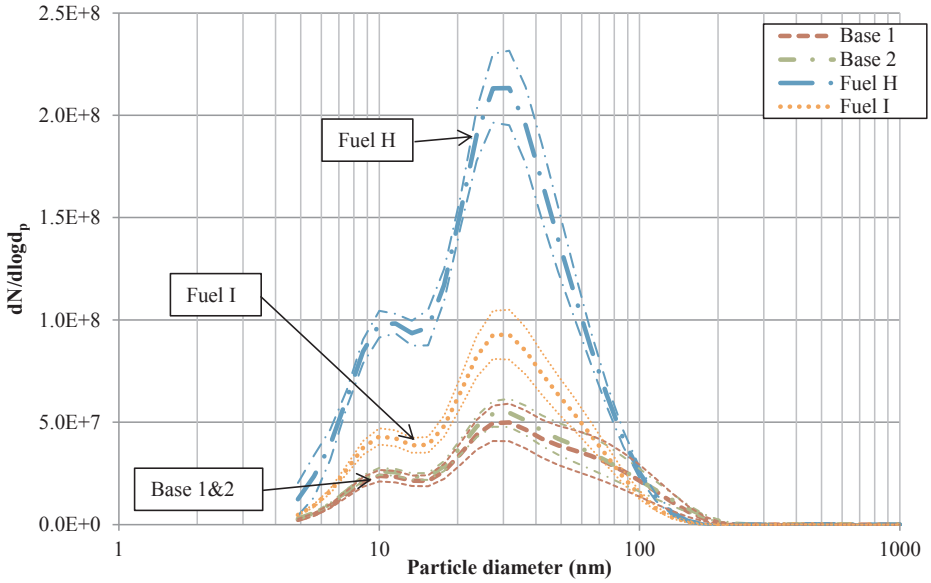

Fig. 5. PN size distributions from market representative fuels at 2000 rpm/full load, (10% EGR) – this corresponds to the patterned bars on Fig. 4. An accumulation mode peak at 30 nm is observed for all fuels. The error bands correspond to ± σ.

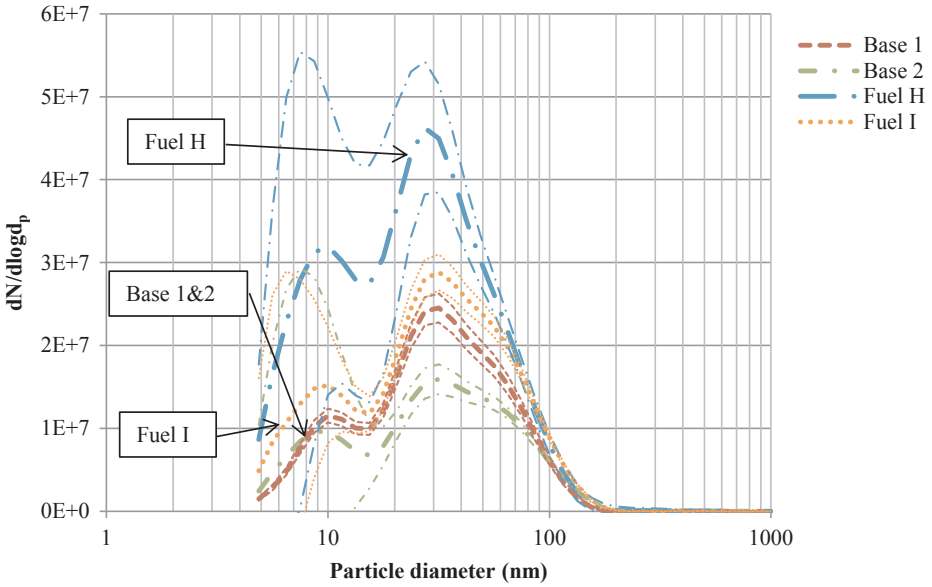

Fig. 7. PN size distributions from market representative fuels at 3000 rpm/full load, (2.2 barA EBP) – this corresponds to the patterned bars on Fig. 6. An accumulation mode peak at 30 nm is observed for all fuels. The error bands correspond to ± σ.

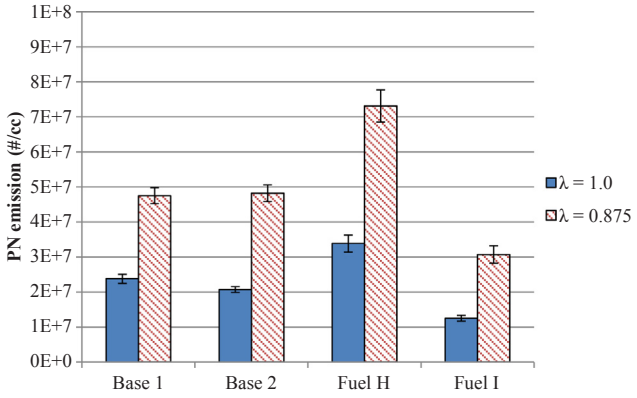

Fig. 8. PN emissions from market representative fuels at 4000 rpm/full load – showing the effect of decreasing lambda from 1.0 to 0.875. The error bars correspond to ± σ.

observed with highly boosted engines, with a nucleation mode peak at 10 nm and an accumulation mode peak at around 30 nm clearly visible. The repeatability of the base fuel between runs is observed to be excellent. At this test point, Fuel H emits the most particles, with Base and Fuel I emitting similar levels.

3.4. 3000 rpm/full load (Test point 3)

Fig. 6 shows the PN emissions from the market representative fuels at 3000 rpm/full load, as the exhaust back-pressure (EBP) is increased from 1.7 to 2.2 barA (mimicking the transition from supercharged to turbocharged operation) and Fig. 7 presents the size distributions from the 2.2 barA case. Fuels H, and I do not exhibit a significant difference in PN emissions as the EBP is increased, unlike the Base fuel. It would be expected that increasing EBP would increase in-cylinder residuals and so promote spray evaporation and hence reduce PN emissions; it is not known why these fuels do not follow this trend as significantly as the Base fuel does. In Fig. 7 the accumulation mode peak at ~ 30 nm from all fuels can be seen.

3.5. 4000 rpm/full load (Test point 4)

Fig. 8 shows the PN emissions from the market representative fuels at 4000 rpm/full load, and Fig. 9 gives the size distributions. As expected, a rich mixture leads to a significant increase in PN emissions from all three of these fuels.

3.6. Specially blended test fuels

Seven fuels were tested which were specially blended for a variety of purposes and are not representative of commercially available fuels. As previously mentioned, four fuels (A-D) represented a “deconvolved” RON-MON matrix with broadly independent RON and MON as far as was possible within the blending limits. Two fuels had been specially blended to vary laminar burning velocity, fuels E (a fast burning fuel) and F (a slow burning fuel). Fuel G is a special fuel with an artificially boosted RON to the extremely high level of 111.6. Fuels A and B contain MTBE, an oxygenate; none of the other specially blended test fuels contained any oxygenate components. Fuels A, C, D, E, F, and G have notably different distillation curves to the market fuels, as can be seen in [29,30] and so would be expected to have a different evaporative performance upon injection and hence different PN emissions.

3.7. 1250 rpm/3.77 bar BMEP (Test point 2)

Fig. 10 shows the PN emissions from the specially blended test fuels at 1250 rpm/3.77 bar BMEP – the NEDC minimap point. The size distributions at this test point are shown in Fig. 11 and show a nucleation mode peak at 30 nm (except Fuel G – see below) and an accumulation mode peak at ~105 nm for Fuels B, E, and F, and at ~250 nm for Fuels A, C, D, and G; this is typical of what might be seen from an unboosted engine. Fuel G emits the largest number of particles by around an order of magnitude, however, looking at the size distribution in Fig. 11, it can be seen that it is emitting a very large number of particles smaller than 40 nm, which (even with the digital filtering) account for almost all of its PN emission in Fig. 10. Fuels B, E, and F emit around two orders of magnitude higher PN than Fuels A, C, and D.

The expected reduction in PN with increase in inlet air temperature is noted for Fuels A, C, D and G, however Fuels B, E, and F show a small increase in PN emissions as inlet air temperature increases. Fuels E and F have a very low final boiling point (FBP) (around 50 °C lower than the

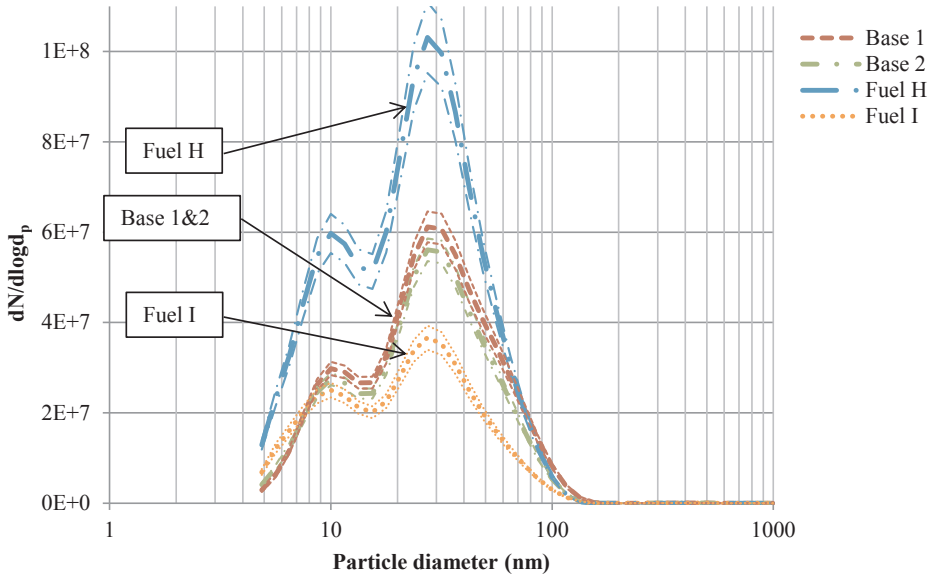

Fig. 9. PN size distributions from market representative fuels at 4000 rpm/full load, (λ = 1.0) – this corresponds to the solid bars on Fig. 8. An accumulation mode peak at 30 nm is observed for all fuels. The error bands correspond to ± σ.

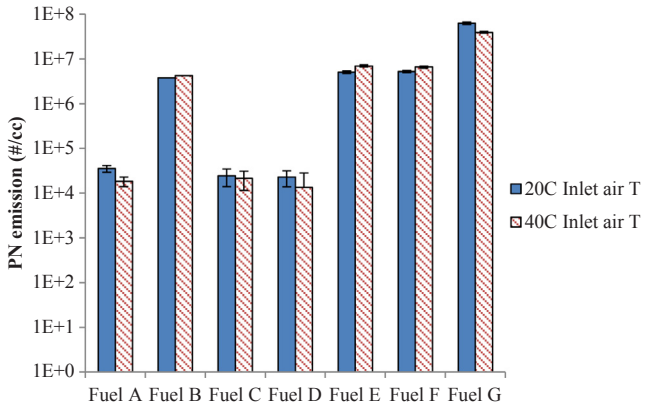

Fig. 10. PN emissions from specially blended test fuels at 1250 rpm/3.77 bar BMEP – showing the effect of increasing inlet air temperature from 20 °C to 40 °C. The error bars correspond to ± σ. Note the logarithmic scale on the ordinate.

other fuels tested), so it may be that the FBP is low enough that the fuel is fully evaporated even with the inlet air temperature at 20 °C. Fuel B has a vapour pressure that is very high and it is possible that this trend is similar to that seen with Fuel I in Fig. 2, namely that the high vapour pressure is leading to very fast evaporation of Fuel B on injection and hence a locally rich, less homogeneous mixture, leading to an overall increase in PN emissions.

3.8. 2000 rpm/full load (Test point 1)

Fig. 12 shows the PN emissions from the specially blended test fuels at 2000 rpm/full load with 0% and 10% cooled, external EGR, Fig. 13 shows the size distributions. Here, Fuel B emits the highest number of particles by a factor of 2 or so. Of interest here is the fact that increasing EGR from 0% to 10% increases the PN emissions from Fuels A, B, D, E, and G. As would be expected, there is no change in PN from Fuel F, and there is a noticeable reduction (by a factor of 2) in the emissions from Fuel C. With every fuel, adding EGR reduced the exhaust temperature by around 40 °C, reducing post-flame oxidation and hence leading to an increase in PN emissions, which makes the result from Fuel C all the more surprising.

The size distribution (Fig. 13) shows again the standard bimodal distribution expected at this boosted condition for all seven fuels, with a nucleation mode peak at ~ 10 nm and an accumulation mode peak at ~ 30 nm, it also shows that Fuel D emits very low levels of PN across the size distribution. The previously observed high levels of sub-40 nm particles for Fuel G are not observed at this test condition.

3.9. 3000 rpm/full load (Test point 3)

Fig. 14 shows the PN emissions from the specially blended test fuels at 3000 rpm/full load varying the exhaust back pressure from 1.7 barA to 2.2 barA and Fig. 15 the size distribution. At this test condition the results noted at the other test conditions are followed closely, and as has been previously noted there is a small reduction in PN emissions with increasing exhaust back pressure. This reduction is due to the increase in in-cylinder residuals increasing the charge temperature, promoting spray evaporation and hence decreasing PN emissions. Of note here is that Fuels E and F have significantly different PN emissions, with Fuel E, a fuel with a higher laminar flame speed giving lower PN emissions than Fuel F – this effect is observed both at this test point and the other full load test points. Fig. 15 shows again similar mode shapes and sizes to the other test conditions with Fuels B and F having a wide nucleation mode extending to ~100 nm; the very high levels of very small particles from Fuel G that were seen at Test Point 2 are again noted here.

3.10. 4000 rpm/full load (Test point 4)

Fig. 16 shows the PN emissions from specially blended test fuels at 4000 rpm/full load varying lambda from 1.0 to 0.875 and the size distributions are shown in Fig. 17. Similar trends between the fuels are observed at this test point with Fuels B, F, and G emitting the highest number of particles, as at 3000 rpm. As expected, a rich mixture leads to a significant increase in PN emissions from all seven of these fuels. Looking at the size distributions (Fig. 17), the standard boosted distribution is again noted. The high levels of particles emitted by Fuel G are further explained by the size distribution, where it can be seen that Fuels B and G emit almost the same level of PN except below 20 nm where Fuel G emits significantly more.

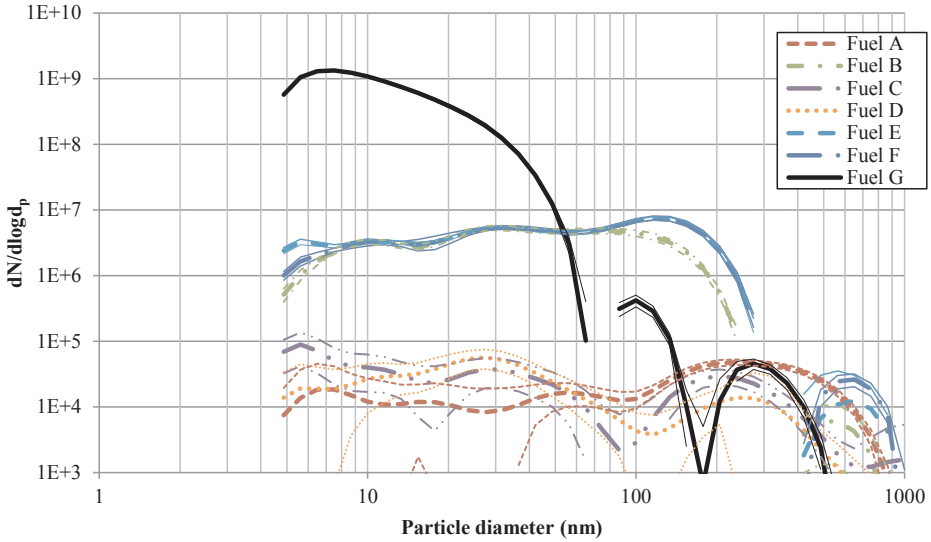

Fig. 11. PN size distributions from specially blended test fuels at 1250 rpm/3.77 bar BMEP, (Inlet air T = 20 °C) corresponding to the solid bars on Fig. 10. The error bands correspond to ± σ.

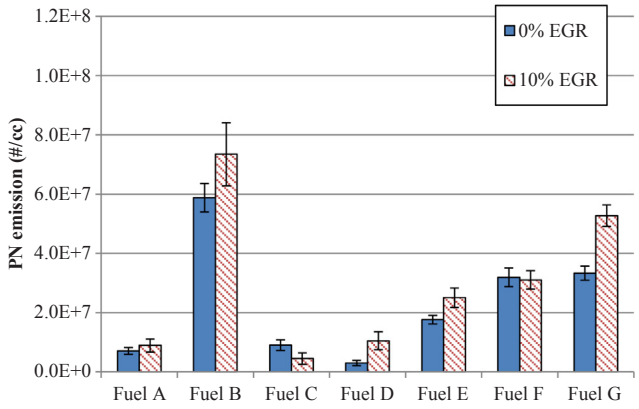

Fig. 12. PN emissions from specially blended test fuels at 2000 rpm/full load – showing the effect of adding EGR. The error bars correspond to ± σ.

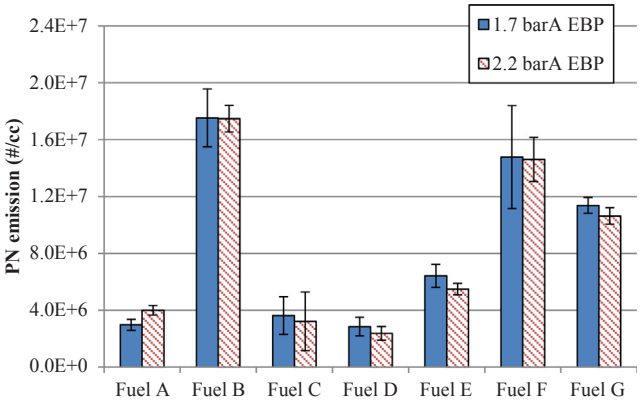

Fig. 14. PN emissions from specially blended test fuels at 3000 rpm/full load – showing the effect of exhaust back pressure. The error bars correspond to ± σ.

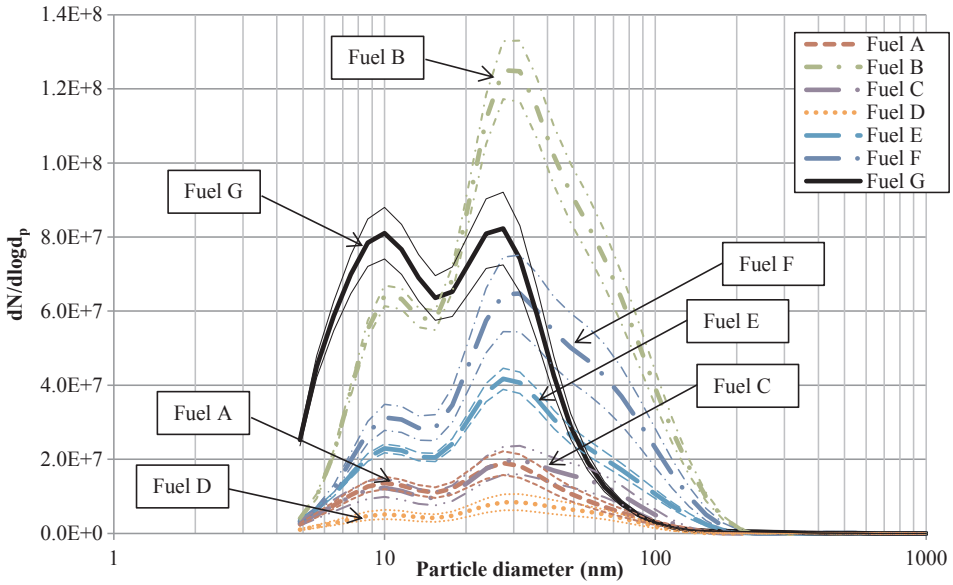

Fig. 13. PN size distributions from specially blended test fuels at 2000 rpm/full load, (0% EGR) corresponding to the solid bars on Fig. 12. The error bands correspond to ± σ.

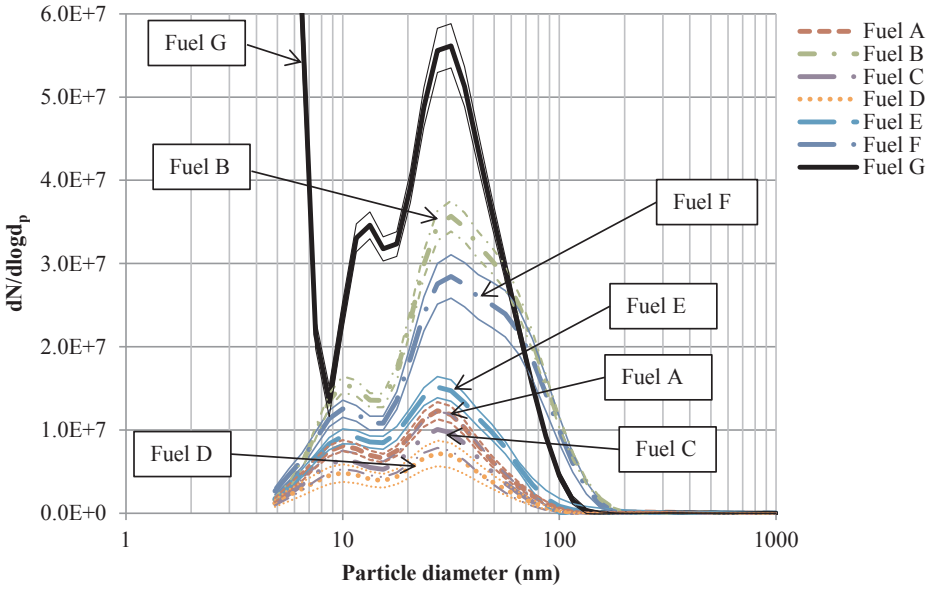

Fig. 15. PN size distributions from specially blended test fuels at 3000 rpm/full load, (EBP = 2.2barA) corresponding to the patterned bars on Fig. 14. The error bands correspond to ± σ.

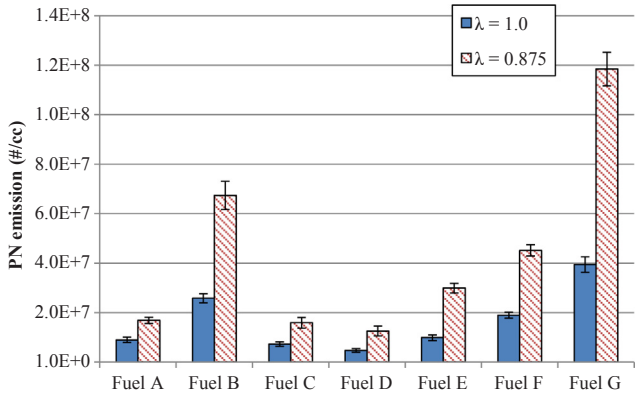

Fig. 16. PN emissions from specially blended test fuels at 4000 rpm/full load – showing the effect of air–fuel ratio. The error bars correspond to ± σ.

4. Discussion

4.1. Small particles

With every fuel tested at boosted conditions (Test Points 1, 3, and 4) an accumulation mode peak at approximately 30 nm has been noted (with a corresponding nucleation mode peak at around 10 nm) and with almost no particles observed above 100 nm. This is consistent with other measurements from boosted GDI engines [8,34] running on standard gasoline. This is the first time such small particles have been observed in engine-out emissions from such a wide range of fuels and has important implications for after treatment. Although we are measuring engine-out emissions, without after treatment, the three-way catalyst (TWC) would only be expected to remove volatile particles, not solid accumulation mode particles [35]. As most global emissions legislation stands (where such legislation restricts the number of particles emitted), there are lower size limits on PN measured. The current EU

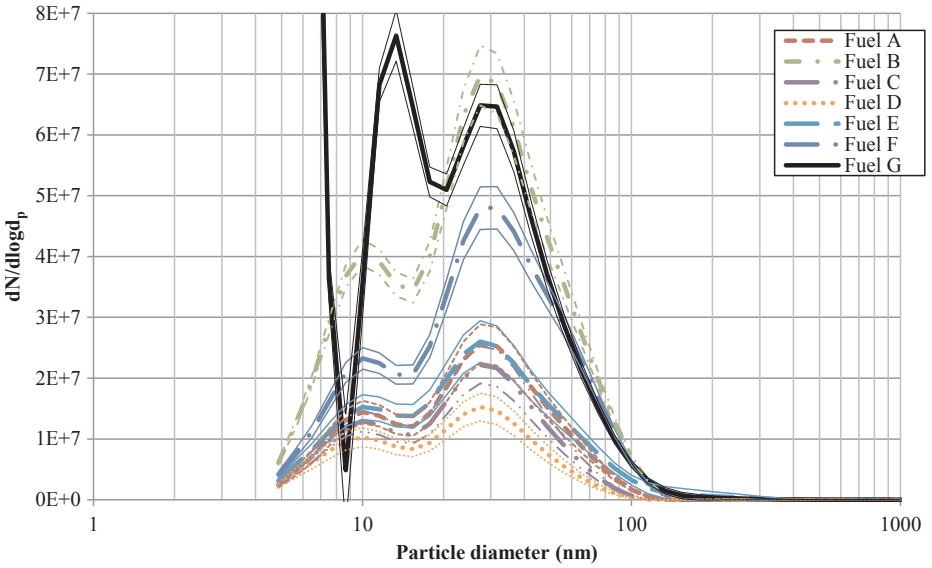

Fig. 17. PN size distributions from specially blended test fuels at 4000 rpm/full load, (λ = 1) corresponding to the solid bars on Fig. 16. The error bands correspond to ± σ.

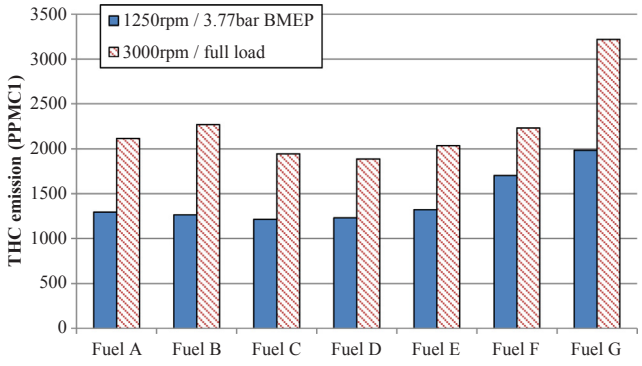

Fig. 18. THC emissions from the specially blended test fuels at two test conditions (1250 rpm/3.77 bar BMEP, 20 °C inlet air T and 3000 rpm/full load, 1.7barA EBP). Very high THC emissions from Fuel G are noted supported by the very high numbers of small particles observed with this fuel (Fig. 11 and Fig. 15).

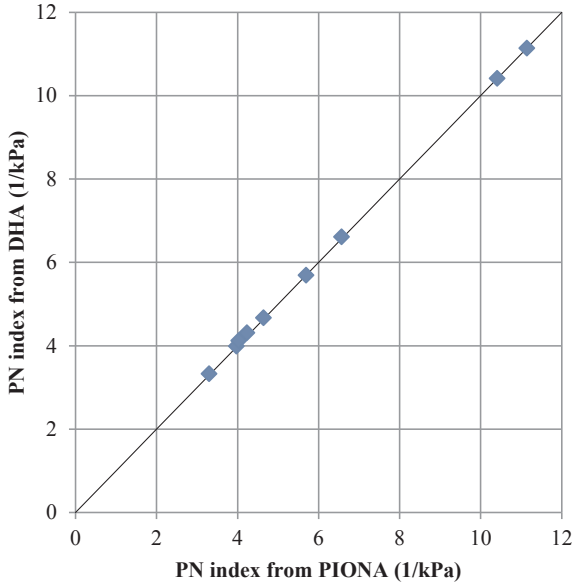

Fig. 19. Comparison of PN index values from PIONA and DHA results (the unity slope is also plotted).

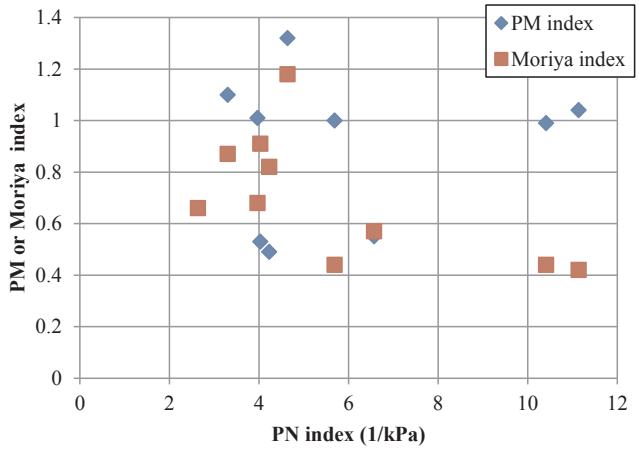

Fig. 20. Comparison between the PN index and PM and Moriya indices.

legislation [22] specifies a count efficiency of 50% at 23 nm and 90% at 41 nm, these diameters are higher than the accumulation mode peak observed in this work.

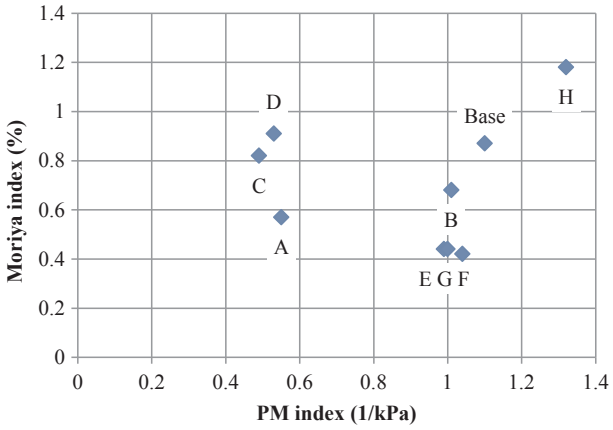

Fig. 21. Comparison between the PM index and Moriya index, the labels refer to the fuel name.

4.2. Fuel G

Fuel G emitted extremely high levels of very small particles at three of the four test points. These are of such a size that it is likely that they are volatile particles. To verify this, the Total Hydrocarbon (THC) emissions of the engine have been measured and are shown in Fig. 18. This clearly shows that the THC emissions from Fuel G are significantly higher than other fuels as well, consistent with the particles observed being volatiles, which would be removed by a standard TWC. In addition, Fuel G had a surprisingly high BSFC [30] for a given level of spark advance which agrees with these observations.

Fuel G has a highly atypical distillation curve, with only 10% (v/v) recovered at 100 °C (as compared to around 60% for the other fuels) [30]. This means that it is much less likely to have fully evaporated at ignition, and indeed surface wetting is much more likely as well. This behaviour will lead to a very inhomogeneous mixture and hence the high levels of PN emissions observed.

It is important to recognise that physical effects that cause a spray to wet the wall can have a bigger effect on particulate emissions than the specific fuel composition. It is known that absence of light ends in a fuel can lead to a longer spray penetration [36] and for Fuel G, the lower volatility leads to greater wall wetting and would appear to explain its higher particulate emissions and relatively poor efficiency. Injector tip deposits can also perturb the spray and are also observed to lead to large increases in PM emissions [37–40].

4.3. Evaluation of indices

4.3.1. Comparison of PN index calculation methods

Due to the DHA that was carried out for all fuels (except fuel I) it is possible to compare the PN index values for these fuels using this more detailed calculation method and that obtained by the standard PIONA analysis. The results of this comparison are shown in Fig. 19 and the raw data is in Table 3. It is clear that there is a very close agreement, with all but two fuels' PN indices within 1%, and none differing by more than 2%. This demonstrates the strength of the PIONA method for calculating the PN index, as even with significantly more information available (from the DHA) the value of the PN index is essentially unchanged.

4.3.2. Comparison between the PM index, PN index, and Moriya index

For the 10 fuels tested here it is interesting to compare the values of the PN, PM, and Moriya index which are obtained. These are shown in Figs. 20 and 21 and the raw data in Table 3. It is interesting to note that there is no clear correlation between any of the three indices for these 10 fuels. This is particularly interesting result, as all three indices have shown potential in predicting particulate emissions from GDI engines,

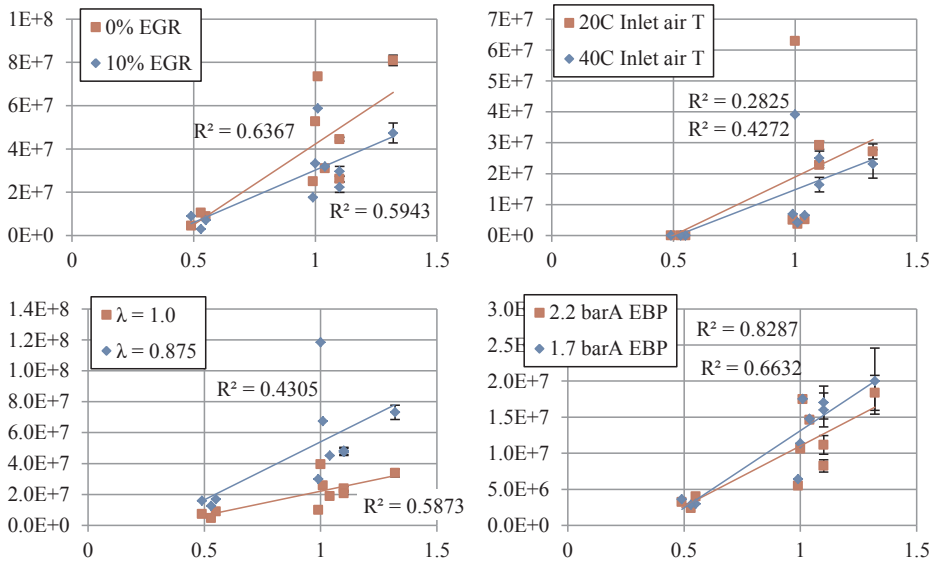

Fig. 22. PN emissions (in #/cc on the abcissa) vs PM index (in 1/kPa on the ordinate) for all fuels (Test points 1–4 clockwise from top left).

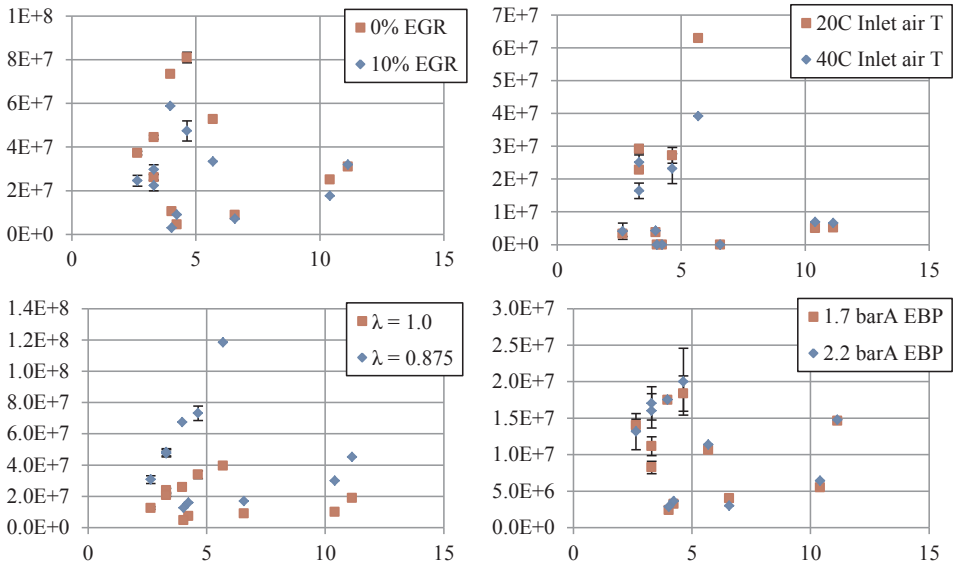

Fig. 23. PN emissions (in #/cc on the abcissa) vs PN index (in 1/kPa on the ordinate) for all fuels (Test points 1–4 clockwise from top left).

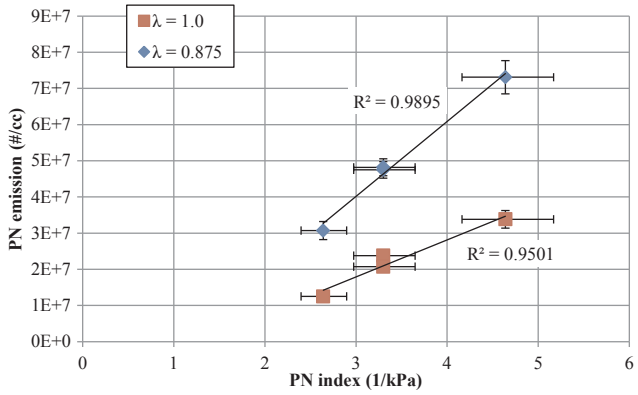

Fig. 24. PN emissions from market representative fuels (Base, H, and I) at 4000 rpm/full load vs PN index. The error bars correspond to ± σ for the particulate results and minimum and maximum values for the PN index.

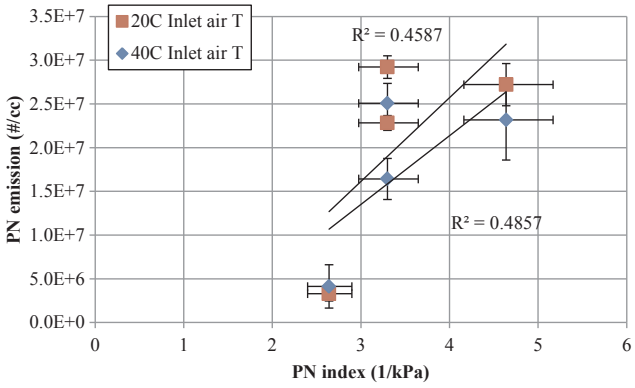

Fig. 25. PN emissions from market representative fuels (Base, H, and I) at 1250 rpm/3.77 bar BMEP vs PN index. The error bars correspond to ± σ for the particulate results and minimum and maximum values for the PN index.

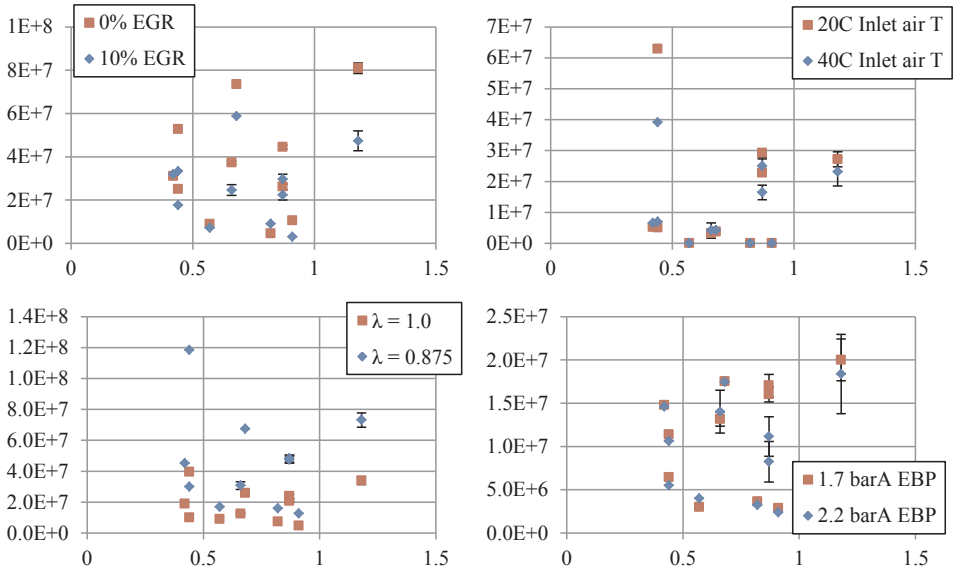

Fig. 26. PN emissions (in #/cc on the abcissa) vs Moriya index (in % on the ordinate) for all fuels (Test points 1–4 clockwise from top left).

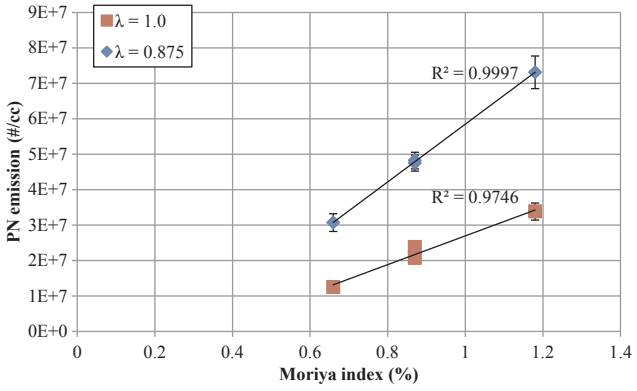

Fig. 27. PN emissions from market representative fuels (Base, H, and I) at 4000 rpm/full load vs Moriya index. The error bars correspond to ± σ.

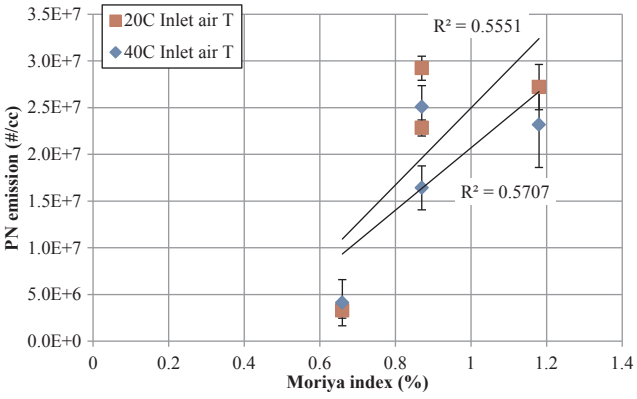

Fig. 28. PN emissions from market representative fuels (Base, H, and I) at 1250 rpm/3.77 bar BMEP vs Moriya index. The error bars correspond to ± σ.

and so it might be hoped that they would show the same trends. All three of the indices assume a linear correlation between the index of the fuel and the PN emissions from that fuel, so when these have been compared, a linear relationship has been assumed and the correlation of that relationship has been evaluated.

4.4. Applicability of the PM index

Fig. 22 presents the PM index vs PN emissions for all four test points (the KLSA case for each). It is striking that in general the PM index is a very good predictor of PN emissions from these 10 fuels at all test points. In all cases the trends are well replicated, although the correlations are rarely strong, and certainly much less strong than has been observed in the literature (R^2 > 0.9 reported) [14,15].

4.5. Applicability of the PN index

Fig. 23 shows the PN index vs PN emissions for all four test points (the KLSA case for each). In this case it is even harder to see a correlation between the Moriya index and the PN emissions than it was with the PN index. Clearly the PN index does not predict PN emissions well from these fuels.

Looking at individual results to understand this lack of correlation, it is noted that at Test point 2 Fuels B, E, and F emit around two orders of magnitude higher PN than Fuels A, C, and D. This behaviour is not predicted by the PN index; Fuels B, E, and F have a higher level of aromatic components (35–40%) compared to Fuels A, C, and D but also a significantly higher VP, this causes their PN index to be lower, however it is likely that these higher levels of aromatics in these fuels are contributing to its high levels of PN emissions. Fuels E&F are notable outliers at all test points in Fig. 23. All of these fuels except Fuels B & G have VPs outside the range that would be acceptable for market fuels (EN228 specifies a minimum of 45 kPa in summer and up to a minimum of 70 kPa in the winter). In addition, as discussed earlier, Fuel G has a very atypical distillation curve, with very few light ends present. This suggests that the PN index may not accurately predict PN emissions from fuels which do not meet market specifications.

The PN index was developed for market representative fuels tested, so it is interesting to check its applicability to those fuels in this study, in particular the distillation curves of the specially blended test fuels are different to those of the market fuels, and therefore their evaporative performance and hence PN emissions on injection would be expected to be different. Fig. 24 shows the correlation between the PN index and the PN emitted from the market fuels on this engine is very high, with R^2s > 0.95 at 4000 rpm/full load.

However, taking the same set of fuels at a different test condition, the PN index is a much less reliable predictor. Fig. 25 shows the PN emissions vs PN index for the market fuels on this engine at 1250 rpm/

3.77 bar BMEP, the trend is still a strong positive, however the correlation is much less good, with R^2 around 0.5.

4.6. Applicability of the Moriya index

Fig. 26 shows the Moriya index vs PN emissions for all four test points (the KLSA case for each). In this case it is even harder to see a correlation between the Moriya index and the PN emissions than it was with the PN index. With these 10 fuels, overall the Moriya index seems not to predict PN emissions from them well.

However, again restricting the comparison to market representative fuels, the results show a very good correlation again, this time between the Moriya index and the PN emissions. This is shown in Figs. 27 and 28. Here the correlations are very similar, even slightly stronger than those for the PN index.

The PM Index requires a Detailed Hydrocarbon Analysis but does in general appear to be a more accurate predictor of particulate emissions than the PN index or Moriya index. For each component the Double Bond Equivalent and the VP at 443 K, both need to be determined in order to assess the overall contribution to the index. It is found that heavier aromatics (C9 +) make a significant contribution to the PM Index because they have a DBE of 4, but also they have a low vapour pressure at 443 K. This effect is less apparent in the other indices because they use distillation parameters relating to the whole fuel, and the influence of particular components is less apparent.

5. Conclusions

PN emissions from a highly boosted engine operating at BMEPs up to 35 bar with 10 different test fuels have been measured for the first time. Fuel composition remains an important factor in the particulate emissions from a highly boosted engine compared to engines with more usual levels of boost; however it is not the only significant parameter. The effects of fuel composition have been shown to vary as other combustion parameters have been changed – for example the addition of EGR caused some fuels to emit more particulates, and others to emit less. Indeed the effects of fuel composition also changed as engine operating point changed in some cases. Other physical properties of fuels can also be important in circumstances where less volatile fuels can cause increased wall wetting.

This work has also compared three common particulate indices, the PM, PN, and Moriya indices, against the particulate emissions observed from the Ultraboost engine. The following conclusions are drawn:

1. The PM index is a very good predictor of PN emissions from this engine at all test conditions, albeit with lower correlations than have been reported elsewhere [14,15].
2. The PN index and Moriya index do not predict the PN emissions from all fuels however, when the fuels are restricted to those representative of market fuels then both predict the PN emissions well. This shows that a simple index is not always the best predictor, particularly outside the area in which it has been developed.
3. The PN index and Moriya index are simple indices, calculable from information available on a standard fuel specification. The PM index, on the other hand, is more complex and requires a DHA to be calculated. It is therefore not surprising that the more information that is known about a fuel, the better one is able to predict its PN emissions.
4. The PM index is closely related to the heavy aromatic content in the fuel. This relationship is not as apparent in the other indices.

The measurement of small accumulation mode particles, with all fuels, at boosted conditions has significant implications for after treatment and legislation which in current form, considers particles larger than the very small (~30 nm) particles observed here. It would be of interest to further investigate these very small particles to further understand their structure.

Acknowledgments

The authors acknowledge the Technology Strategy Board (now Innovate UK), the UK's innovation agency, for the partial funding of this work. Consortium members GE Precision Engineering, Lotus Engineering, CD-Adapco, Imperial College London, and the University of Leeds have all made various portions of this work possible.

Funding

This work was funded by Jaguar Land Rover, Shell, and the Technology Strategy Board (now Innovate UK). In addition, all of the project partners listed above made contributions. Felix Leach acknowledges the support of an EPSRC studentship and partial support from EP/I011331/1.

Appendix A. Supplementary data

Supplementary data to this article can be found online at https://doi.org/10.1016/j.fuel.2019.04.115.

References

[1] Gasoline Direct Injection (GDI) System Market Size By Component (Electronic Control Units, Fuel Injectors, Fuel Pumps, Sensors), By Application (Passenger Car [PC], Commercial Vehicle [CV]), Industry Analysis Report, Regional Outlook (U.S., Canada, Germany, UK, France, Italy, China, Japan, South Korea, India, Brazil, Mexico), Application Potential, Competitive Market Share & Forecast, 2016 – 2024. In: Global Market Insights; 2017.
[2] Zhao H. Overview of gasoline direct injection engines. Advanced direct injection combustion engine technologies and development: gasoline and gas engines. Woodhead Publishing Ltd; 2010.
[3] Friedfeldt R, Zenner T, Ernst R, Fraser A. Three-cylinder gasoline engine with direct injection. Auto Tech Review 2013;2:32–7.
[4] Eastwood P. Particulate emissions from vehicles. SAE International and John Wiley & Sons Ltd; 2008.
[5] Stone CR. Introduction to internal combustion engines. 4th ed. Palgrave Macmillan; 2012.
[6] Raza M, Chen L, Leach F, Ding S. A review of particulate number (PN) emissions from gasoline direct injection (GDI) engines and their control techniques. Energies 2018;11:1417.
[7] Peckham MS, Finch A, Campbell BW, Price P, Davies M. Study of Particle Number Emissions from a Turbocharged Gasoline Direct Injection (GDI) Engine Including Data from a Fast-Response Particle Size Spectrometer, in: SAE 2011 World Congress & Exhibition, April 2011, SAE, Detroit, MI, USA; 2011.
[8] Bonatesta F, Chiappetta E, La Rocca A. Part-load particulate matter from a GDI engine and the connection with combustion characteristics. Appl Energy 2014;124:366–76.
[9] Oh C, Cheng WK. Assessment of gasoline direct injection engine cold start particulate. Emission Sources 2017.
[10] Leach F, Stone R, Richardson D, Lewis A, Akehurst S, Turner J, et al. Particulate emissions from a highly boosted Gasoline Direct Injection engine. Int J Engine Res 2018;19:347–59.
[11] Hashimoto K, Inaba O, Akasaka Y. Effects of fuel properties on the combustion and emission of direct-injection gasoline engine. SAE International; 2000.
[12] Chapman E, Winston-Galant M, Geng P, Latigo R, Boehman A. Alternative Fuel Property Correlations to the Honda Particulate Matter Index (PMI), in: SAE International Powertrains, Fuels & Lubricants Meeting, SAE International; 2016.
[13] Wittmann J-H, Menger L. Novel index for evaluation of particle formation tendencies of fuels with different chemical compositions. SAE Int J Fuels Lubr 2017;10.
[14] Aikawa K, Sakurai T, Jetter JJ. Development of a predictive model for gasoline vehicle particulate matter emissions. SAE Int J Fuels Lubr 2010;3:610–22.
[15] Aikawa K, Jetter JJ. Impact of gasoline composition on particulate matter emissions from a direct-injection gasoline engine: applicability of the particulate matter index. Int J Engine Res 2014;15:298–306.
[16] Law CK. Combustion physics. 1st ed. Cambridge: Cambridge University Press; 2006.
[17] ASTM, D5134 – Standard Test Method for Detailed Analysis of Petroleum Naphthas through n-Nonane by Capillary Gas Chromatography; 2017.
[18] Leach F, Richardson D, Stone R. The Influence of Fuel Properties on Particulate Number Emissions from a Direct Injection Spark Ignition Engine, SAE 2013 World Congress & Exhibition, 2013-01-1558; 2013.
[19] Leach F, Stone R, Fennell D, Hayden D, Richardson D, Wicks N. Predicting the particulate matter emissions from spray-guided gasoline direct-injection spark ignition engines. Proc Inst Mech Eng Part D: J Automobile Eng 2017;231:717–30.
[20] B. Standards, BS EN 13016-1:2007 Determination of air saturated vapour pressure (ASVP) and calculated dry vapour pressure equivalent (DVPE), in, 2007.

[21] ASTM, D1319 – Standard Test Method for Hydrocarbon Types in Liquid Petroleum Products by Fluorescent Indicator Adsorption, in.
[22] Commission Regulation 692/2008, OJ L 199 of 18.7.2008, in.
[23] Moriya H. Fuel Property Influence on Exhaust Emissions – Simplified PM Index. In: SAE-China Congress & Exhibition, Shanghai; 2016.
[24] Leach F, Knorsch T, Laidig C, Wiese W. A review of the requirements for injection systems and the effects of fuel quality on particulate emissions from GDI engines. In: International Powertrain, Fuels, and Lubricants meeting, SAE, Heidelberg; 2018.
[25] Barrientos EJ, Anderson JE, Maricq MM, Boehman AL. Particulate matter indices using fuel smoke point for vehicle emissions with gasoline, ethanol blends, and butanol blends. Combust Flame 2016;167:308–19.
[26] Turner J, Popplewell A, Patel R, Johnson T, Darnton N, Richardson S, et al. Ultra boost for economy: extending the limits of extreme engine downsizing. SAE Int J Engines 2014;7.
[27] Reavell K, Hands T, Collings N. A Fast Response Particulate Spectrometer for Combustion Aerosols. In: SAE Powertrain & Fluid Systems Conference & Exhibition, October 2002, SAE, San Diego, CA, USA, 2002.
[28] Braisher M, Stone CR, Price P. Particle Number Emissions from a Range of European Vehicles, SAE Technical Paper, 2010-01-0786; 2010.
[29] Remmert S, Campbell S, Cracknell R, Schuetze A, Lewis A, Giles K, et al. Octane appetite: the relevance of a lower limit to the MON specification in a downsized, highly boosted DISI engine. SAE Int J Fuels Lubr 2014;7:743–55.
[30] Remmert S, Cracknell R, Head R, Schuetze A, Lewis A, Akehurst S, et al. Octane response in a downsized, highly boosted direct injection spark ignition engine. SAE Int J Fuels Lubr 2014;7:131–43.
[31] Leach FCP, Stone R, Richardson D, Turner JWG, Lewis A, Akehurst S, et al. The effect of oxygenate fuels on PN emissions from a highly boosted GDI engine. Fuel 2018;225:277–86.
[32] Andersson J, Giechaskiel B, Muñoz-Bueno R, Sandbach E, Dilara P. Particle measurement programme (PMP) light-duty inter-laboratory correlation exercise (ILCE_LD) final report. European Commission Joint Research Centre Institute for Environment and Sustainability; 2007.
[33] Mohd Murad SH, Camm J, Davy M, Stone R, Richardson D, Spray,. Behaviour and particulate matter emissions with M15 methanol/gasoline blends in a GDI engine. SAE International; 2016.
[34] Karjalainen P, Pirjola L, Heikkilä J, Lähde T, Tzamkiozis T, Ntziachristos L, et al. Exhaust particles of modern gasoline vehicles: a laboratory and an on-road study. Atmos Environ 2014;97:262–70.
[35] Chen L, Braisher M, Crossley A, Stone R, Richardson D. The Influence of Ethanol Blends on Particulate Matter Emissions from Gasoline Direct Injection Engines. In: SAE 2010 World Congress & Exhibition, SAE International, Detroit, Michigan, United States; 2010.
[36] van Romunde Z, Aleiferis PG, Cracknell RF, Walmsley HL. Effect of fuel properties on spray development from a multi-hole DISI engine injector. SAE International; 2007.
[37] Henkel S, Hardalupas Y, Taylor A, Conifer C, Cracknell R, Goh TK, et al. Injector Fouling and Its Impact on Engine Emissions and Spray Characteristics in Gasoline Direct Injection Engines; 2017.
[38] Badawy T, Attar MA, Hutchins P, Xu H, Krueger Venus J, Cracknell R. Investigation of injector coking effects on spray characteristic and engine performance in gasoline direct injection engines. Appl Energy 2018;220:375–94.
[39] Jiang C, Xu H, Srivastava D, Ma X, Dearn K, Cracknell R, et al. Effect of fuel injector deposit on spray characteristics, gaseous emissions and particulate matter in a gasoline direct injection engine. Appl Energy 2017;203:390–402.
[40] Wang C, Xu H, Herreros JM, Wang J, Cracknell R. Impact of fuel and injection system on particle emissions from a GDI engine. Appl Energy 2014;132:178–91.